parasitologia

MDPI

Article

Hirsutonosema embarrassi n. gen. n. sp. (Phylum Microsporidia) in the Ovary of Mucket (*Actinonaias ligamentina*), Plain Pocketbook (*Lampsilis cardium*), and Fatmucket (*Lampsilis siliquoidea*) (Unionidae) from the Embarrass River, Wisconsin, USA †

Susan Knowles [1,*], Eric M. Leis [2], Jordan C. Richard [3,4], Isaac F. Standish [2], Jamie Bojko [5,6], Jesse Weinzinger [7] and Diane L. Waller [8]

1 National Wildlife Health Center, U.S. Geological Survey, Madison, WI 53711, USA
2 La Crosse Fish Health Center-Midwest Fisheries Center, U.S. Fish and Wildlife Service, Onalaska, WI 54650, USA; eric_leis@fws.gov (E.M.L.); sirisaac_standish@fws.gov (I.F.S.)
3 Freshwater and Marine Sciences Program, Department of Pathobiological Sciences, University of Wisconsin-Madison, Madison, WI 53711, USA; jcrichard2@wisc.edu or jordan_richard@fws.gov
4 Southwestern Virginia Field Office, U.S. Fish and Wildlife Service, Abingdon, VA 24210, USA
5 National Horizons Centre, Teesside University, Darlington DL1 1HG, UK; j.bojko@tees.ac.uk
6 School of Health and Life Sciences, Teesside University, Middlesbrough TS1 3BX, UK
7 Wisconsin Department of Natural Resources, Wisconsin Rapids, WI 54494, USA; jesse.weinzinger@wisconsin.gov
8 Upper Midwest Environmental Sciences Center, U.S. Geological Survey, La Crosse, WI 54603, USA; dwaller@usgs.gov
* Correspondence: sknowles@usgs.gov
† urn:lsid:zoobank.org:act:3D108B67-A304-4A7E-A60E-D61087808E80.

check for updates

Citation: Knowles, S.; Leis, E.M.; Richard, J.C.; Standish, I.F.; Bojko, J.; Weinzinger, J.; Waller, D.L. *Hirsutonosema embarrassi* n. gen. n. sp. (Phylum Microsporidia) in the Ovary of Mucket (*Actinonaias ligamentina*), Plain Pocketbook (*Lampsilis cardium*), and Fatmucket (*Lampsilis siliquoidea*) (Unionidae) from the Embarrass River, Wisconsin, USA. *Parasitologia* **2024**, *4*, 184–198. https://doi.org/10.3390/parasitologia4020016

Academic Editor: Geoff Hide

Received: 5 April 2024
Revised: 3 May 2024
Accepted: 7 May 2024
Published: 7 June 2024

Copyright: © 2024 by the authors. Licensee MDPI, Basel, Switzerland. This article is an open access article distributed under the terms and conditions of the Creative Commons Attribution (CC BY) license (https://creativecommons.org/licenses/by/4.0/).

Abstract: During an epidemiological survey following a mortality event of freshwater mussels in 2018 in the Embarrass River, Wisconsin, USA, we identified a novel microsporidian parasite in the ovaries of mucket (*Actinonaias ligamentina*), plain pocketbook (*Lampsilis cardium*), and fatmucket (*Lampsilis siliquoidea*) (Unionidae). Histopathology showed round-to-oval microsporidian spores in the cytoplasm of oocytes in 60% (3/5) of female mucket, 100% (4/4) of female plain pocketbook, and 50% (1/2) of female fatmucket. Using transmission electron microscopy, we found that mature spores were round-to-oval and measured 4.13 ± 0.64 µm (3.14–5.31) long by 2.88 ± 0.37 µm (2.36–3.68) wide. The spores had a thin electron-dense exospore with a spiky "hairy" coat, a thick electron lucent endospore, diplokaryotic nuclei, a polar vacuole, and 27–28 polar filaments arranged in 1–3 rows. Sequencing of the small subunit rRNA produced a 1356 bp sequence most similar to that of *Pseudonosema cristatellae* (92%), and phylogenetic analysis grouped it within the freshwater Neopereziida. Genetic, morphological, and ultrastructural characteristics did not closely match those of other *Pseudonosema* spp., and a new genus and species, *Hirsutonosema embarrassi* n. gen. n. sp., were designated. Additional studies could evaluate host susceptibility, distribution, seasonality, transmission, and lethal or sub-lethal effects of this parasite on freshwater mussels.

Keywords: *Actinonaias ligamentina*; freshwater mussel; *Hirsutonosema embarrassi* n. gen. n. sp.; histopathology; *Lampsilis cardium*; *Lampsilis siliquoidea*; microsporidia; Neopereziida; TEM; unionid

1. Introduction

North America is home to the richest freshwater mussel fauna in the world, having 302 of the documented 1200 worldwide species [1,2]. In North America, approximately two thirds of freshwater mussel species are considered threatened or near-threatened [2]. Explanations for the causes of mussel declines in the United States have often included pollution and habitat destruction or alteration, as well as the introduction of invasive species, overharvesting, lack of fish hosts, climate change, predation, genetic change,

endocrine disruptors, and disease [3,4]. There are 53 native mussel species in Wisconsin [5], five of which are listed as federally endangered [6], 11 as state-endangered [7], eight as state-threatened [7], five as species of special concern [8], and two as extirpated [8]. A 2019 statewide survey of 99 sites from 21 watersheds conducted by the Department of Natural Resource's Wisconsin Mussel Monitoring Program showed 39 species with fatmucket (*Lampsilis siliquoidea*), spike (*Eurynia dilatata*), plain pocketbook (*Lampsilis cardium*), and giant floater (*Pyganodon grandis*) observed most frequently [9].

Snuffbox (*Epioblasma triquetra*) has been listed as a federally endangered species since 2012 and has experienced an 83% historical decline from its former range in the Wolf River System, Wisconsin [9]. At the end of September 2018, the Wisconsin Department of Natural Resources documented unusually high mortality of mussels, including snuffbox (*E. triquetra*), during an annual survey in the Embarrass River, Wisconsin, USA [9]. As a result of the mortality event, a mussel health investigation was initiated. Here, we describe a novel microsporidian parasite, *Hirsutonosema embarrassi* n. gen. n. sp., infecting the ovary of mucket (*Actinonaias ligamentina*), plain pocketbook (*L. cardium*), and fatmucket (*L. siliquoidea*), identified during this health survey.

Microsporidia are obligate spore-forming parasites of animals, including humans, and microeukaryotes classified within Opisthosporidia (Eukaryota: opisthokonta) in three groups defined by environment (Aquasporidia, Marinosporidia, and Terresporidia) [10]. There are an estimated 1600 species [10], which proliferate by merogony and undergo sporogony to produce an infective spore that is transmitted vertically, horizontally, or by both routes [11]. Life cycles may be direct or indirect [12].

2. Results

2.1. Histopathology

Round-to-oval microsporidian spores were observed in the cytoplasm of oocytes from wild mucket (*A. ligamentina*), plain pocketbook (*L. cardium*), and fatmucket (*L. siliquoidea*). Only a few acini were infected in some mussels, while large numbers were infected in others (Figure 1A). Large numbers of microsporidia filled the cytoplasm of mature oocytes in the acinar lumen and of immature oocytes attached to the acinar wall (Figure 1B). Infected oocytes were occasionally observed within ciliated gonadal ducts (Figure 1C). While infected oocytes were not observed in the gills of any of the examined sections, it is possible that they could be found here as the infected egg travels to the marsupium. In some mussels, spores were free within the ovary, especially in those mussels with degenerating acini (Figure 1D). In these instances, hemocytes were occasionally observed, but we do not know if they were responding to the microsporidian spores or the degenerating acini. Microsporidia were not observed within testes. With Brown and Hopps staining, mature spores stained blue while immature spores stained red (Figure 1E). Giemsa stained the nuclei of the proliferative stages blue (Figure 1F). Mature spores were acid-fast-positive with a Ziehl–Neelsen stain while immature spores did not stain (Figure 1G). The polar cap, at the anterior end of spores, stained magenta with the periodic acid–Schiff (PAS) technique (Figure 1H).

Microsporidian spores were present in the ovaries of 100% of plain pocketbook (*L. cardium*), 60% of mucket (*A. ligamentina*), 50% of fatmucket (*L. siliquoidea*), and in no fragile papershell (*Potamilus fragilis*), pink heelsplitter (*Potamilus alatus*), or deertoe (*Truncilla truncata*; Tables 1 and S1). Of the female mussels, 100% of fatmucket (*L. siliquoidea*), 80% of mucket (*A. ligamentina*), 50% of plain pocketbook (*L. cardium*) and deertoe (*T. truncata*), 25% of pink heelsplitter (*P. alatus*), and no fragile papershell (*P. fragilis*) were gravid (Table 1). Of the gravid females, 100% of plain pocketbook (*L. cardium*), 50% of mucket (*A. ligamentina*) and fatmucket (*L. siliquoidea*), and no pink heelsplitter (*P. alatus*) or deertoe (*T. truncata*) were infected (Table 1).

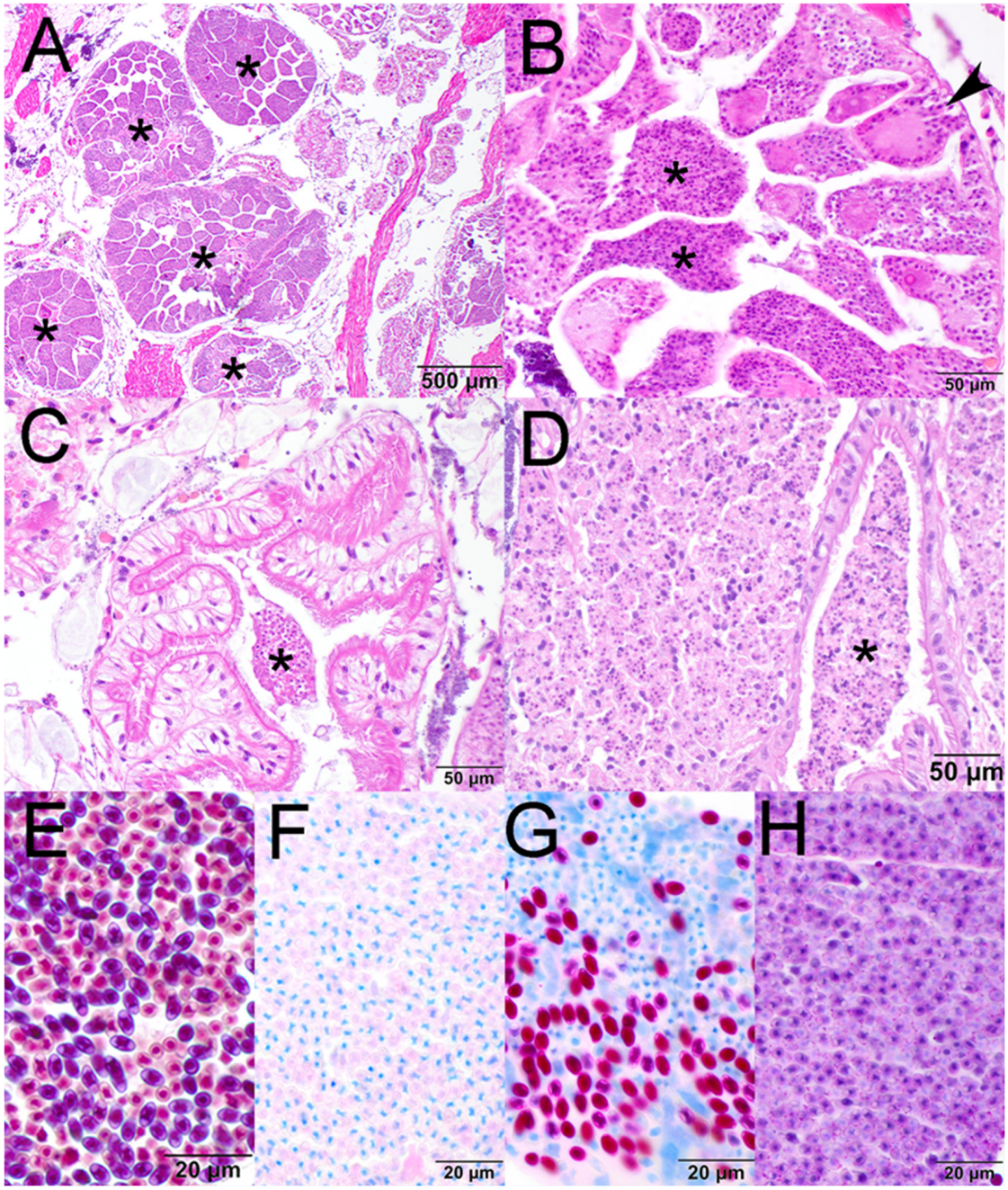

Figure 1. Photomicrographs from the ovaries of mucket (*Actinonaias ligamentina*) and plain pocketbook (*Lampsilis cardium*) collected from the Embarrass River, Wisconsin, USA. (**A**) Low magnification of the ovary of a mucket (*A. ligamentina*) showing multiple acini with microsporidial-infected oocytes (asterisk; hematoxylin and eosin [H&E]); (**B**) an ovarian acinus of a mucket (*A. ligamentina*), with microsporidial-infected mature oocytes in the lumen (asterisk) and infected immature oocytes attached to the acinar wall (arrowhead; H&E); (**C**) an infected oocyte (asterisk) present in the lumen of a ciliated gonadal duct of a mucket (*A. ligamentina*; H&E); (**D**) microsporidia are free within the ovary of this plain pocketbook (*L. cardium*) and within the cytoplasm of an oocyte (asterisk) in a ciliated gonadal duct (H&E); (**E**) mature spores stained blue while immature spores stained red with Brown and Hopps staining; (**F**) Giemsa stained the nuclei of the proliferative stages blue; (**G**) mature spores stained magenta with Ziehl–Neelsen staining; (**H**) the polar cap stained magenta with the periodic acid–Schiff (PAS) technique.

Table 1. Number of freshwater mussels collected from the Embarrass River, Old Mill Park, Wisconsin, USA, on 5 October 2018 infected with *Hirsutonosema embarrassi* n. gen. n. sp. by sex and species.

Species	Number of Males (M), Females (F), Undetermined (U)	Infected	Prevalence in Females	Gravid Females	Prevalence in Gravid Females
Actinonaias ligamentina	4M 5F	3/9	60% (3/5)	4/5	50% (2/4)
Lampsilis cardium	4F	4/4	100% (4/4)	3/4	100% (3/3)
Potamilus fragilis	1F 1U	0/2	0% (0/1)	0/1	NA
Lampsilis siliquoidea	1M 2F	1/3	50% (1/2)	2/2	50% (1/2)
Potamilus alatus	4F	0/4	0% (0/4)	1/4	0% (0/1)
Truncilla truncata	5M 2F	0/7	0% (0/2)	1/2	0% (0/1)
Totals	**10M 18F 1U**	**8/29**	**44% (8/18)**	**11/18**	**55% 6/11**

2.2. Transmission Electron Microscopy

Transmission electron microscopy (TEM) of a formalin-fixed paraffin-embedded sample from a mucket (*A. ligamentina*) showed various stages of merogony and sporogony (Figure 2A). Cell division occurs in the proliferative stage, called merogony. Meronts have few organelles other than the cisternae of endoplasmic reticulum and numerous ribosomes [13]. The surface of meronts may vary from a thin membrane to an electron-dense coat, which may be surrounded by cisternae of host endoplasmic reticulum in late merogony [13,14]. Meronts observed in the cytoplasm of the oocytes had a thin membrane surrounded by cisternae of rough endoplasmic reticulum, and diplokaryotic nuclei with multiple nucleoli (Figure 2B). In sporogony, sporonts divide into sporoblasts and then mature to spores. At the end of merogony, electron-dense material is deposited on the plasma membrane [14]. This stage was not observed. Sporonts are differentiated from meronts by an electron-dense surface coat on the plasma membrane [15]. In the mussel, sporonts had a moderately dense plasma membrane with a short spiky "hairy" coat and diplokaryotic nuclei surrounded by rough endoplasmic reticulum (Figure 2C). Sporoblasts undergo morphogenesis to form spores [15]. The early sporoblasts had a thin electron-dense exospore with a spiky "hairy" coat, diplokaryotic nuclei surrounded by rough endoplasmic reticulum, and 14 polar filaments arranged in 1–2 rows (Figure 2D). The late sporoblasts had undulating walls with a thin electron-dense exospore with a spiky "hairy" coat, a thin developing electron-lucent endospore, diplokaryotic nuclei surrounded by rough endoplasmic reticulum, and 27–28 polar filaments arranged in 1–3 rows (Figure 2E). The mature spores measured 4.13 ± 0.64 µm (range = 3.14–5.31) long by 2.88 ± 0.37 µm (range = 2.36–3.68) wide (n = 14) with a 0.13 ± 0.04 µm (range = 0.1–0.28) wall (n = 14). Tissue processing involved the use of ethanol for dehydration and could have induced spore shrinkage, so the actual spore size could have been larger than reported. Fresh spores were not available for measurements. The spores had a thin electron-dense exospore with a spiky "hairy" coat, a thick electron-lucent endospore, diplokaryotic nuclei, a polar vacuole, and 27–28 polar filaments arranged in 1–3 rows (Figure 2F).

2.3. Molecular Identification

We sequenced a 1356 bp sequence of small subunit (SSU) rRNA for *H. embarrassi* n. gen. n. sp. from the type host *A. ligamentina* (GenBank accession number: PP777264). While not identical to any entries in GenBank, the closest BLAST results were as follows: *Pseudonosema cristatellae* (AF484694.1; 92.36%; e-value = 0; host: the freshwater bryozoan *Cristatella mucedo*), Microsporidia sp. (MT622752.1; 88.79%; e-value = 0; host: the freshwater dipteran *Kiefferulus barbatitarsis*), Microsporidia sp. (MT622753.1; 88.72%; e-value = 0; host: the freshwater dipteran *K. barbatitarsis*), and *Janacekia tainanus* (MW537817.1; 88.72%; e-value = 0; host: the freshwater dipteran *Kiefferulus tainanus*). Other BLAST results sharing lesser similarities were microsporidians with hosts from the phyla annelida, mollusca, nematoda, arthropoda, and bryozoa (Table 2). Our sequence shared 87.03% identity with *Knowlespora clinchi* (OL117026.1; e-value = 0; host: the freshwater mussel *Actinonaias*

pectorosa). The sequence obtained for *H. embarrassi* n. gen. n. sp. from *L. cardium* (GenBank accession number: PP777265) was identical to the sequence obtained from the type host, except a couple of ambiguous base pairs were present. Samples obtained from *L. siliquoidea* were confirmed as being positive for *H. embarrassi* n. gen. n. sp. using the newly developed qPCR assay.

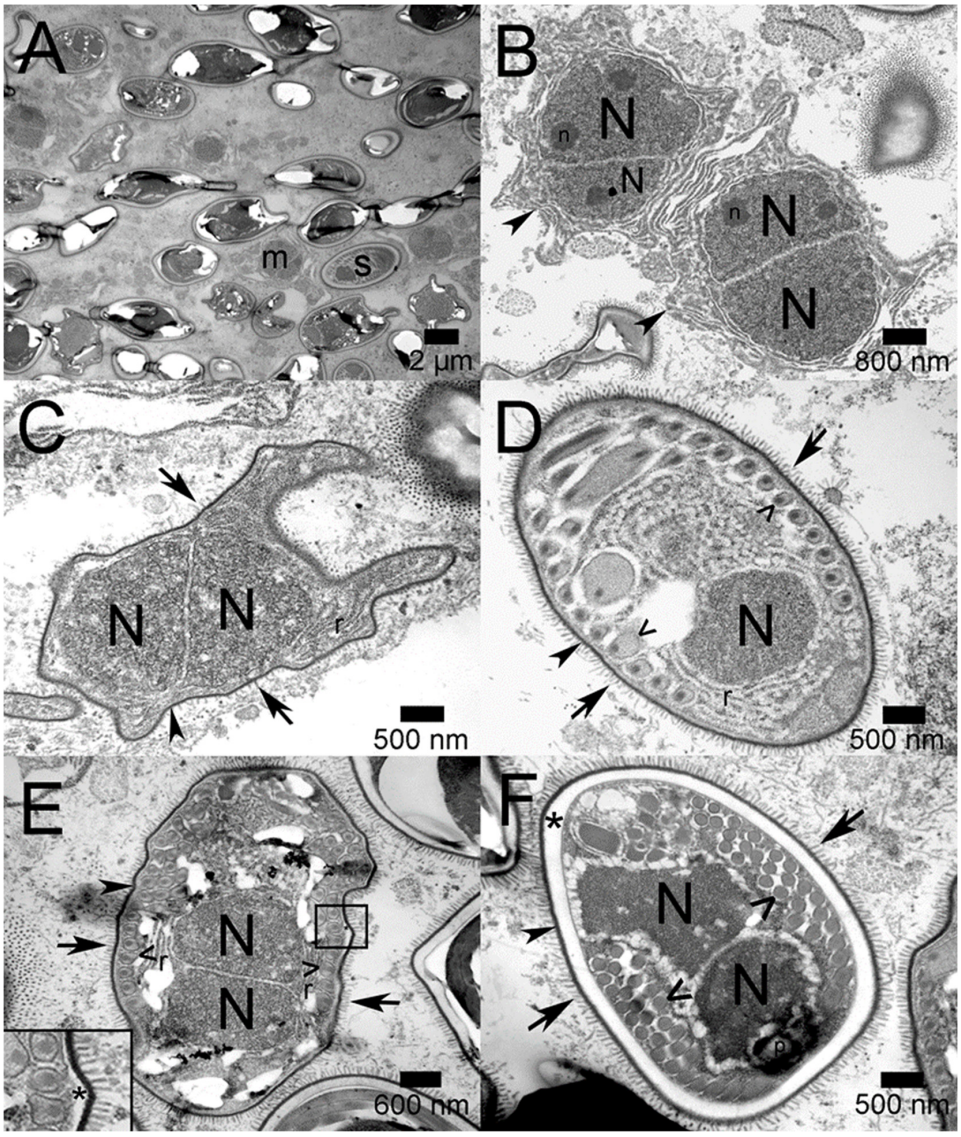

Figure 2. Transmission electron micrographs of the ovary of a wild mucket (*Actinonaias ligamentina*) collected from the Embarrass River, Wisconsin, USA: (**A**) various stages of merogony (m) and sporogony (s) within the cytoplasm of an oocyte; (**B**) meront surrounded by an endoplasmic reticulum (arrowheads) with diplokaryon (N) with multiple nucleoli (n); (**C**) sporont with a moderately dense plasma membrane (arrowhead) with a short spiky "hairy" coat (arrows), and diplokaryon (N) surrounded by rough endoplasmic reticulum (RER) (r); (**D**) early sporoblast with a thin electron-dense exospore (arrowhead) with a spiky "hairy" coat (arrows), one nucleus of the diplokaryon (N) surrounded by RER (r), and 14 polar filaments (carets) arranged in 1–2 rows; (**E**) late sporoblast with undulating wall with a thin electron-dense exospore (arrowhead) with a spiky "hairy" coat (arrows), thin developing electron-lucent endospore (asterisk), diplokaryotic nuclei (N) surrounded by RER (r), and 27–28 polar filaments (carets) arranged in 1–3 rows. Inset: higher magnification of endospore (asterisk); (**F**) mature spore with a thin electron dense exospore (arrowhead) with a spiky "hairy" coat (arrows), thick electron-lucent endospore (asterisk), diplokaryotic nuclei (N), polar vacuole (p), and 27–28 polar filaments (carets) arranged in 1–3 rows.

Table 2. Closest BLAST results to *Hirsutonosema embarrassi* n. gen. n. sp. with an e-value of 0 by species and GenBank accession, percent identity, host and phylum, tissue infected, spore shape, spore size in µm, number of polar filament coils and rows, and exospore layers. The asterisk indicates measurement is an approximation from the publication figure.

Species/GenBank Accession Number	Percent Identity	Host (Phylum)	Tissue Infected	Spore Shape and Size in µm	Polar Filament Coils and Rows	Exospore Layers	Publication
Hirsutonosema embarrassi	100	*Actinonaias ligamentina*, *Lampsilis cardium*, *Lampsilis siliquoidea* (Mollusca)	Ovary	Round-to-oval 4.1 × 2.88	27–28 1–3	1 with a spiky "hairy" coat	This paper
Pseudonosema cristatellae AF484694.1	92.36	*Cristatella mucedo* (Bryozoa)	Epithelial cells of body wall	Broadly pyriform 7.3 × 5.1	22–32 1–4	1	[16,17]
Microsporidia sp. MT622752.1, MT622753.1	88.79 88.72	*Kiefferulus barbatitarsis* (Arthopoda)	Adipose tissue	NA	NA	NA	NA
Janacekia tainanus MW537817.1	88.72	*Kiefferulus tainanus* (Arthropoda)	Adipose tissue	Oval 6.1 × 3.7	13–17 1	1 with tubular secretions	[18]
Jirovecia branchilis OP234512.1, OP234513.1	88.49 88.42	*Branchiura sowerbyi* (Annelida)	Glands	Rod-like 26.6 × 1.8	Manubrium NA	1 in a polar sac	[19]
Bacillidium vesiculoformis AJ581995.1	87.85	*Nais simplex* (Annelida)	Intestinal hemocytes	Cylindrical 12.2 × 1.6	Manubrium NA	1 covered in spherical granules	[20]
Knowlespora clinchi OL117026.1	87.03	*Actinonaias pectorosa* (Mollusca)	Gonad	Round-to-oval 4.6 × 3.7	~13–14 1–2	1	[21,22]
Bacillidium sinensis ON054957.1	87.18	*Branchiura sowerbyi* (Annelida)	Coelomocytes	Rod-like 15.9 × 2.5	Manubrium NA	16	[23]
Nematocenator marisprofundi JX463178.1	84.63	*Desmodora marci* (Nematoda)	Muscle	Pyriform ~8.5 × 2.7 *	3–5 1	1	[24]
Jirovecia sinensis MN752318.1, MN752317.1	88.48 88.36	*Branchiura sowerbyi* (Annelida)	Coelom	Rod-like 17 × 2	Manubrium NA	1 in a polar sac/s	[25]
Bacillidium branchilis ON054958.1, ON054959.1	87.35 86.98	*Branchiura sowerbyi* (Annelida)	Coelomocytes	Rod-like 9.8 × 1.7	Manubrium NA	2	[23]
Microsporidium sp. BPAR4 FJ756101.1	86.38	*Dorogostaiskia parasitica* (Arthropoda)	NA	NA	NA	NA	NA
Schroedera airthreyi AJ749819.1	87.39	*Plumatella* sp. (Bryozoa)	Cells of body wall	Ovoid 8.7 × 5.8	37–38 1–2	2	[26]
Neoperezia chironomid HQ396519.1	86.98	*Chironomus plumosus* (Arthropoda)	Adipose tissue	Wide oval 6.1 × 3.4	24–27 1–3	1	[27]

Table 2. *Cont.*

Species/GenBank Accession Number	Percent Identity	Host (Phylum)	Tissue Infected	Spore Shape and Size in µm	Polar Filament Coils and Rows	Exospore Layers	Publication
Trichonosema pectinatellae AF484695.1	86.89	*Pectinatella magnifica* (Bryozoa)	Coelomic cell	Elongated pyriform 9.5 × 4.5	25 1–3	1 with surface spikes	[16]
Neoperezia semenovaiae HQ396520.1	86.27	*Chironomus plumosus* (Arthropoda)	Adipose tissue	Wide oval 6.0 × 3.5	17–32 1–4	2	[27]
Bryonosema plumatellae AF484692.1, AF484691.1	86.29 85.62	*Plumatella nitens* (Bryozoa)	Coelomic cells	Broadly pyriform 8.4 × 5.8	≤33 1–3	1	[16]
Neoperezia semenovaiae MN512230.1	86.27	NA	NA	NA	NA	NA	NA
Neoperezia semenovaiae MN512229.1	86.15	NA	NA	NA	NA	NA	NA
Trichonosema algonquinensis AY582742.1	86.13	*Pectinatella magnifica* (Bryozoa)	Epithelial cells	Ovoid 8.5 × 4.4	20–33 1–2	1 with finger-like processes	[28]
Schroedera plumatellae AY135024.1	84.50	*Plumatella fungosa* (Bryozoa)	Testes	Oval 7.2 × 5.0	22–23 1–3	1 with bubble-like extensions near poles	[29]
Janacekia debaisieuxi AY090070.1	84.00	*Odagoamia ornuta (Arthropoda)*	NA	NA	NA	NA	[30]
Janacekia debaisieuxi AJ252950.1	83.88	*Simulium equinum* or *S. ornatum* (Arthropoda)	NA	NA	NA	NA	[31]
Bacillidium sp. AF104087.1	83.82	*Lumbriculus* sp. (Annelida)	Coelomocytes	Long-slender 24–27.2 × 3.2	Manubrium NA	NA	[32]

2.4. qPCR

The qPCR assay appeared sensitive and exhibited low variability. Both intra-assay and inter-assay variation appeared low, with coefficients of variation (CV) of <3% down to 10 copies per reaction (Table 3). The assay's limit of detection (LOD) was determined to be 10 copies as the assay could detect all replicates (20 of 20) containing 100 copies, 20 of 20 replicates containing 10 copies, and 5 of 20 replicates (25%) containing 1 copy. Similarly, the limit of quantification (LOQ) was determined to be 10 copies because the starting quantity (SQ) CV in replicate reactions containing more than 10 copies was <20% and increased to 34.64% in reactions containing 1 copy (Table 4).

Table 3. qPCR inter and intra-assay variation. The table shows average quantification cycle (Cq), standard deviation (SD), and coefficient of variation values (CV) of triplicate quantitative polymerase chain (qPCR) reactions of the gBlock® standard curve composed of 10-fold dilutions ranging from 10^7 to 1 copy per reaction. Reactions containing one copy exhibited insufficient amplification for determination (NA).

gBlock® Copies	C_q Mean	C_q Mean SD	C_q CV (%)
Intra-assay			
10,000,000	17.37	0.28	1.60
1,000,000	20.30	0.13	0.63
100,000	23.73	0.29	1.21
10,000	26.98	0.36	1.32
1000	30.19	0.28	0.94
100	34.07	0.27	0.78
10	37.31	0.72	1.93
1	39.50	NA	NA
Inter-assay			
10,000,000	17.16	0.35	2.02
1,000,000	20.17	0.22	1.08
100,000	23.65	0.31	1.31
10,000	26.83	0.40	1.49
1000	30.16	0.30	0.99
100	33.87	0.37	1.10
10	37.20	0.66	1.77
1	39.91	0.79	1.97

Table 4. qPCR limit of quantification (LOQ). The LOQ was determined by running eight replicates of a standard curve of gBlock® (10^7 to 1 copy per reaction). Standard values were assigned to four replicates, and the remaining replicates were used to calculate the mean starting quantity (SQ), standard deviation (SD), and coefficients of variation (CV).

gBlock® Copies	SQ Mean	SQ SD	SQ CV (%)
10,000,000	11,935,000.00	948,063.82	7.94
1,000,000	1,063,125.00	78,387.16	7.37
100,000	80,337.50	11,217.60	13.96
10,000	6697.50	468.25	6.99
1000	530.50	29.02	5.47
100	44.56	8.81	19.77
10	26.24	1.92	7.34
1	1.47	0.51	34.64

2.5. Taxonomic Description

2.5.1. Higher Taxonomy

Superphylum: Opisthosporidia [33].
Phylum: Rozellomycota [34], including the Microsporidia [35].
Class: Aquasporidia [36].
Order: Neopereziida [10].
Family: Neopereziidae [37].
Genus: *Hirsutonosema* Knowles, Leis, Richard, Standish, Bojko, Weinzinger, Waller 2024.

Genus description: Species belonging to the genus *Hirsutonosema* should be 90–100% similar to the SSU gene sequence available for the type species (*Hirsutonosema embarrassi*: GenBank PP777264) of this genus. Phylogenetically, candidate species should clade with the type species using SSU phylogenetics. Phenotypic plasticity is known to occur within Microsporidia, increasing the chance of variability within genera; however, similar developmental characteristics (lack of a sporophorous vesicle) and morphological features [spiky "hairy" exospore coat; polar filament coils (n = ≥27); and nuclei count (n = 2)] increase taxonomic confidence. The host range for this genus includes molluskan bivalve hosts.

Species: *Hirsutonosema embarrassi* n. gen. n. sp. Knowles, Leis, Richard, Standish, Bojko, Weinzinger, Waller.

Species description and diagnosis: Organisms within the *Hirsutonosema embarrassi* species should be 98–100% similar at the SSU gene (GenBank PP777264) and group phylogenetically with the type species. This species includes microsporidian parasites that infect oocytes of freshwater bivalves, particularly those in the Lampsilini tribe Ihering, 1901 including *A. ligamentina*, *L. cardium*, and *L. siliquoidea*. A histologic examination showed round-to-oval spores that partially or completely filled the cytoplasm of immature and mature oocytes. Merogony and sporogony occur in direct contact with the cytoplasm of the host. With transmission electron microscopy, mature spores measured 4.1 µm long and 2.9 µm wide with a 0.17 µm thick spore wall. There was a minimum of 27 polar filaments and a diplokaryotic mature spore.

2.5.2. Taxonomic Summary

Type host: *A. ligamentina* (Mucket).
Other hosts: *L. siliquoidea* (Fat Mucket); *L. cardium* (Plain Pocketbook).
Site of infection: Cytoplasm of oocytes.
Type locality: Embarrass River, Wisconsin, USA (44.739844° N; 88.798594° W).
Prevalence in type host: three of five females.
Specimens deposited: Hapantotype slides of stained gonadal tissue were deposited in the Smithsonian National Museum of Natural History (Washington, DC, USA) under accessions USNM 1607135 (host: *A. ligamentina*), USNM 1607136 (host: *L. cardium*), and USNM 1607137 (host: *L. siliquoidea*).
Etymology: This genus name is in regard to morphology as the Latin word hirsute means "hairy", which describes the appearance of the exospore coat. The species name is in reference to the type locality.
DNA sequences: Partial SSU rRNA genes were submitted to GenBank under Accessions PP777264 (host: *A. ligamentina*; 1356 bp) and PP777265 (host: *L. cardium*; 1206 bp).

2.5.3. Remarks upon the Taxonomic Summary

The microsporidian observed in the ovary of three unionid mussel species in the Embarrass River, Wisconsin, USA clearly belonged to a novel genus. The spores of *H. embarrassi* n. gen n. sp. were round to oval and generally similar in size to those of *K. clinchi*, a species previously described from the gonads of pheasantshell mussels (*A. pectorosa*) in the Clinch River, USA [21,22]. However, the two species were not similar genetically (~87% with SSU rRNA gene) and can easily be separated morphologically, as the latter species lacks a spiky "hairy" coat on the exospore and has fewer polar filament coils (Table 2). While exospore adornments are useful in separating *Hirsutonosema* n. gen. and *Knowlespora*, exospore adornments have also been reported in the following genetically similar taxa: *J. tainanus*, *Bacillidium vesiculoformis*, *Trichonosema algonquinensis*, and *Schroedera plumatellae*. *Hirsutonosema embarrassi* n. gen. n. sp. can be separated from these through differences observed in genetics, host species, tissue tropism, spore morphology, and the number of polar filament coils (Table 2). This new species represents the second described genus and species known to infect the reproductive tissues of freshwater mussels.

2.6. Phylogeny

A maximum-likelihood phylogeny using the SSU sequence from *H. embarrassi* n. gen. n. sp. places it within the Neopereziida order and within the "freshwater" cluster of this order (Figure 3). This novel isolate clades most closely with *P. cristatellae* with strong bootstrap support (100%); however, the bootstrap support of the topology above this grouping was low (68%). A second freshwater mussel microsporidian (*K. clinchi*) also branches closely to this new isolate but is represented by its own distinct branch at low support (68%). Another known mussel microsporidian (*Steinhausia* sp.; marine) clades within Enterocytozoonida, a different order from the one in which *H. embarrassi* n. gen. n.

sp. presents in our topology. The differences between these three mussel-infecting species are also represented by low levels of sequence similarity, where *K. clinchi* is 87% similar overall to the new isolate, and Steinhausia is 71% similar.

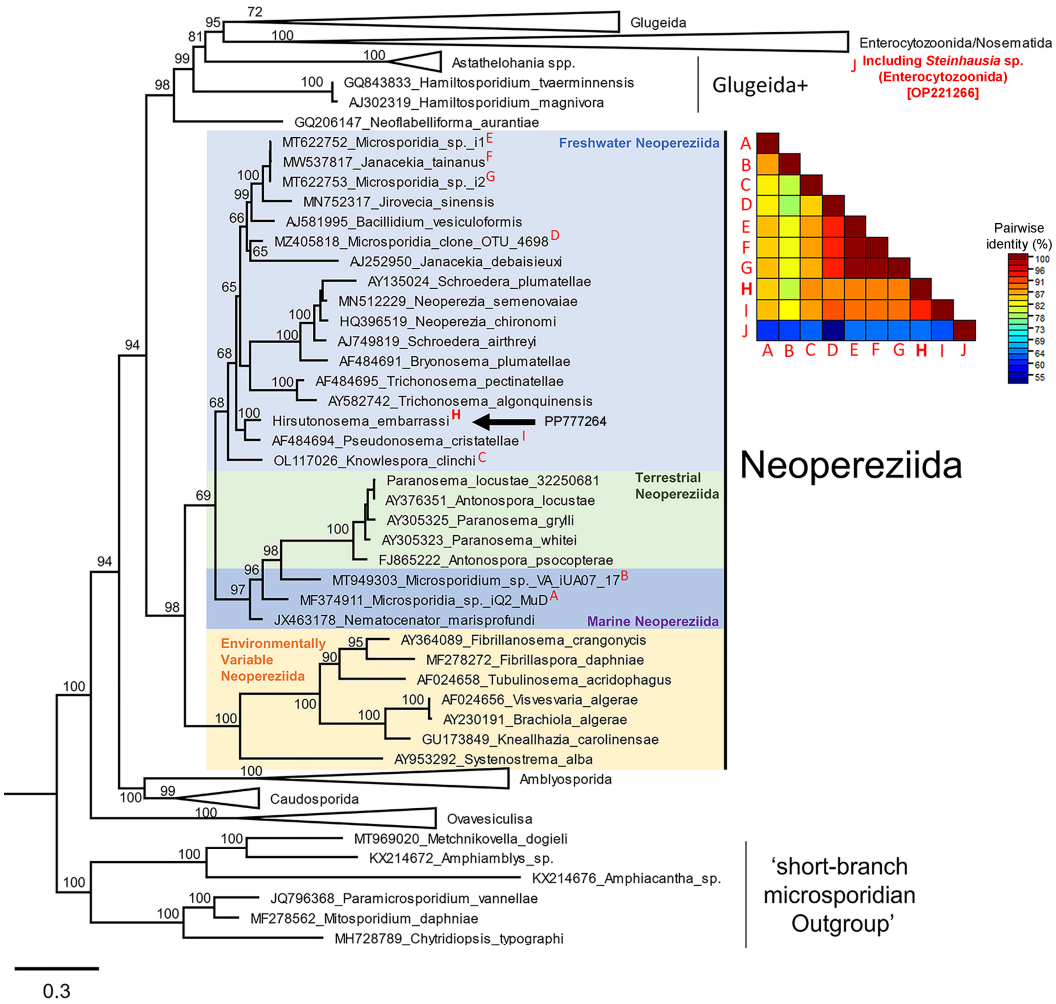

Figure 3. A maximum-likelihood phylogenetic tree comprising > 100 microsporidian species, representing all currently classified genera, following the phylogeny presented in Bojko et al. [10], with the addition of *Hirsutonosema embarrassi* n. gen. n. sp. (this study), *Steinhausia* sp. (OP221266) from an alternative study [38], and several microsporidian sequences within 10% similarity of the *H. embarrasi* SSU. The phylogeny included 4631 comparable columns and was compared using the best-fitting GTR + F + I + G4 model, according to the Bayesian Information Criterion. The tree was produced using IQ-Tree [39] and visualized and annotated using FigTree v.1.4.4. In addition to the phylogeny, a demarcation plot is provided, comparing similar sequences and other microsporidians from molluskan hosts.

3. Discussion

Historically, microsporidian taxonomy was based on lifecycle, morphology, host range and tissue tropism, but expanded molecular and genomic information has allowed for revised species identification and phylogeny [10]. Phylogenetically, *H. embarrassi* n. gen. n. sp. is most closely related to *P. cristatellae* (92.36%) and falls within the group freshwater Neopereziida (Figure 3). Neopereziida encompasses 29 characterized species that occur predominantly in terrestrial or freshwater environments of the Northern Hemisphere, infecting bryozoans, crustaceans, insects, oligochaetes, and mammals [10]. Infections may be systemic or localized to adipose tissue, gonads, lymphoid or blood cells, and muscle. There is wide variation in spore size, morphology, and transmission.

Three species of Microsporidia are known to infect bivalves. Infections with the microsporidian *Steinhausia* sp. have been reported in the ovaries of marine bivalves, with *Steinhausia mytilovum* first observed in *Mytilus edulis* [40], and *Steinhausia ovicola* first observed in *Ostrea edulis* [41]. Ovarian *Steinhausia*- and *Steinhausia*-like infections have been described in the Baltic clam (*Macoma balthica*) [42], the clam *Venerupis corrugata* (synonym: *Venerupis pullastra*) [43], the Sydney rock oyster (*Saccostrea glomerata*; synonym: *Saccostrea commercialis*) [44], the common cockle (*Cerastoderma edule*) [45,46], and oysters (*Crassostrea tulipa*; synonym: *Crassostrea gasar*) in Brazil [47]. There was a single report of a gonadotropic microsporidian parasite, *K. clinchi*, in the freshwater mussel *A. pectorosa* (Unioinidae) [21,22]. The only available sequence data for *Steinhausia* spp. are from that of *S. mytilovum* from a Mediterranean mussel (*Mytilus galloprovincialis*) [38], which shares 71% identity with *H. embarrassi* n. gen. n. sp. *Hirsutonosema embarrassi* n. gen. n. sp. shares only 87% similarity to *K. clinchi*., the only known microsporidian of freshwater mussels.

While the BLAST matches for *H. embarrassi* n. gen. n. sp. (Table 2) were only reported in a single-host species, three of the six mussel species examined in our study were infected with *H. embarrassi* n. gen. n. sp. The host range of most microsporidians is narrow, and they typically infect only one or closely related host species or species within a group or clade; however, a few species such as *Enterocytozoon bieneusi* are generalists with broad host ranges [48]. In marine bivalves, *S. mytilovum* and *S. ovicola* infect bivalves belonging to the families Mytilidae and Ostreidae, respectively [38]. All mussels in this study fall within the Lampsilini tribe, but only three of the six were infected. It is possible that additional sampling could reveal that all of these species are infected with *H. embarrassi* n. gen. n. sp. Host range can also be broader when the host is immunocompromised [48], and this may warrant further investigation in mussels from this river. Some host species can be infected with multiple microsporidia, as seen with the oligochaete worm, *Branchiura sowerbyi* (Table 2). The microsporidians in this study shared the same tissue tropism with infections occurring within the ovary in the three infected species. Of the closest matches, only *S. plumatellae* was found in the gonads (testes), while other matches were found in epithelial cells, adipose tissue, glands, hemocytes, coelomocytes, and muscle (Table 2).

While the microsporidians in this study were round-to-oval, similar to those of *K. clinchi*, the spore shape of the closest matches varied from pyriform to oval to rod-like to cylindrical to slender. The spore sizes of the matches varied widely from 4.6–27.2 µm × 1.5–5.8 µm with the size of *H. embarrassi* n. gen. n. sp. being most closely related to *K. clinchi*. In comparison to *H. embarrassi* n. gen. n. sp. with 27–28 polar filament coils in 1–3 rows, the number of polar filament coils and rows in the matches varied from 3–38 and 1–4, respectively, with some spores lacking polar filament coils and instead having a manubrium. The number of layers in the exospore varied widely with some spores having only one layer while *Bacillidium sinensis* showed sixteen. *Hirsutonosema embarrassi* n. gen. n. sp. had only one layer in its exospore, but the exospore had a spiky "hairy" coat similar to that of *Trichonosema pectinatellae*. Exospore adornments in the form of tubular secretions, spherical granules, finger-like processes, and bubble-like extensions were present in *J. tainanus*, *B. vesiculoformis*, *T. algonquinensis*, and *S. plumatellae*, respectively. While *P. cristatellae* shared the highest sequence similarity to *H. embarrassi* n. gen. n. sp., the tissue tropism, spore shape, spore size, and exospore differed morphologically. This highlights the importance of using phenotypic and ecological data together with genomic data for microsporidian taxonomy.

Lastly, while an infection with *H. embarrassi* n. gen. n. sp. was not likely the cause of the high mortality observed in the Embarrass River, Wisconsin, USA, in 2018, which has not recurred, it was likely a stressor in this population, and intense infections could be contributing to low recruitment in this population, which includes the federally endangered snuffbox (*E. triquetra*). While the route of transmission is not known, as for other microsporidia, transmission may occur horizontally when spores are released from eggs or vertically from an infected mussel to its progeny [11]. There is a link between transmission and virulence with horizontal transmission showing a higher parasite burden and pathogenicity and vertical transmission with a lower virulence, which favors female

host survival [12]. However, vertical transmission can result in the death of males or feminization, which affects population sex ratios [12]. In the Embarrass River, horizontal transmission may be occurring between different species. Even if vertical transmission does not occur with *H. embarrassi* n. gen. n. sp., as observed with some species of fish, the degenerating, infected eggs could be a source of infection for viable glochidia in the marsupium [13]. The thick spore wall allows for environmental persistence even when hosts are not present [12], which could affect restoration efforts. If infected adult mussels are used for propagation efforts in hatcheries, the hatchery itself can become infected and progeny used in restoration efforts could be a source of infection for previously uninfected populations. Additional studies to evaluate host range, distribution, seasonality, transmission, and lethal or sub-lethal effects on freshwater mussels may be warranted.

4. Materials and Methods

4.1. Experimental Design and Field Sampling

During October of 2018, we sampled adult mucket (*A. ligamentina*), plain pocketbook (*L. cardium*), fragile papershell (*P. fragilis*), fatmucket (*L. siliquoidea*), pink heelsplitter (*P. alatus*), and deertoe (*T. truncata*) from a single site (44.739844° N; 88.798594° W) in the Embarrass River near Pella, Wisconsin, USA, as part of an epidemiological survey investigating an ongoing mortality event in freshwater mussels. During the investigation, we non-lethally collected hemolymph from mussels to assess the virome and microbiome, and we selected a subset of these mussels for histopathology. Nine *A. ligamentina*, four *L. cardium*, two *P. fragilis*, three *L. siliquoidea*, four *P. alatus*, and seven *T. truncata* were collected for histopathology and molecular assays. At the time of collection, mussels were covered with wet paper towels, sealed in plastic bags, and stored on ice in a cooler for transportation to the laboratory.

4.2. Tissue Processing

Mussels were transported to the U.S. Geological Survey Upper Midwest Environmental Sciences Center (La Crosse, WI, USA) and placed in an aerated tank with flow-through water at 12 °C for 24–72 h for depuration. The posterior portion of the mussel was placed in 10% neutral buffered formalin (NBF) and allowed to fix for at least 24 h. The anterior portion of the mussel was stored frozen at −80 °C for molecular analyses. Formalin-fixed tissues were washed in water, transferred to 70% ethanol, and shipped to the U.S. Geological Survey's National Wildlife Health Center (Madison, WI, USA). A single oblique cross section which included gonad was taken through the visceral mass and placed in 10% NBF before processing at the Wisconsin Veterinary Diagnostic Laboratory as previously described [21]. Select tissues were stained with Gram (Brown and Hopps), Giemsa, and Ziehl–Neelsen stains, and the periodic acid–Schiff (PAS) technique and examined with an Olympus BX43 microscope (Evident Scientific, Inc., Waltham, MA, USA) to visualize microsporidian spores.

4.3. Transmission Electron Microscopy

A paraffin block from a mucket (*A. ligamentina*) infected with microsporidium was processed for transmission electron microscopy at the University of Wisconsin's School of Medicine and Public Health (Madison, WI, USA) using previously described methods [21].

4.4. Molecular Identification

Ovaries from mussels histologically identified as infected with microsporidia were sampled from tissues stored at −80 °C. The tissue was placed in a microcentrifuge tube and the DNA was extracted using a DNeasy Blood and Tissue Kit (Qiagen; Hilden, Germany). The extracted DNA underwent amplification of the SSU rRNA gene using the primers V1F and 1492R [21,49]. Successful PCR reactions were sequenced by Eton Biosciences (Newark, NJ, USA), and the sequences were edited and de novo assembled in Geneious [50]. BLAST

searches in GenBank of the resulting contiguous sequences were used to identify similar species [51,52].

4.5. qPCR Development

Reactions (25 µLs) contained 12.5 µL of PrimeTime Gene Expression Mastermix (IDT; Coralville, IA, USA), 500 nM of the forward primer 5′-GCGGCTTAATTTGACTCAACG-3′, 500 nM of the reverse primer 5′-TTCTGTATTATCTTGGGAATCCTCTC-3′, and 350 nM of the probe 5′-FAM/ACATTCGGC/ZEN/CCTGGTAAGTTGTCC/IABKFQ-3′. The probe contained an Iowa Black® fluorescent quencher (IDT), an FAM fluorophore, and a ZEN internal quencher. Reactions were conducted with the following cycling parameters: 95 °C for 5 min, followed by 45 cycles of 95 °C for 15 s and 55 °C for 1 min.

4.6. Phylogenetics

The SSU sequences for representative microsporidian species from known genera were collected [10], with the addition of newly reported species (e.g., Steinhausia sequence data) and the addition of the new microsporidian sequence to provide a maximum-likelihood phylogenetic tree. The SSU sequences were first aligned using MAFFT (via the CIPRES web server) and then uploaded to IQ-Tree [39], where an evolutionary model was defined using the Bayesian Information Criterion, and a tree topology was estimated using 1000 bootstraps.

Supplementary Materials: The following supporting information can be downloaded at: https://www.mdpi.com/article/10.3390/parasitologia4020016/s1, Table S1: Freshwater mussels collected from the Embarrass River, Wisconsin, USA, by accession number, collection date and location, species, health status, sex, gravidity status, and microsporidia status.

Author Contributions: Conceptualization, S.K., E.M.L., J.C.R., J.W. and D.L.W.; data curation, S.K., E.M.L. and J.C.R.; formal analysis, S.K., E.M.L., J.C.R., J.B. and I.F.S.; funding acquisition, J.C.R., and D.L.W.; investigation, S.K., E.M.L., J.C.R., J.B. and J.W.; methodology, S.K., E.M.L., J.C.R., I.F.S. and D.L.W.; project administration, S.K. and E.M.L.; resources, S.K., E.M.L. and D.L.W.; supervision, D.L.W.; validation, S.K., E.M.L., J.C.R. and J.B.; visualization, S.K. and E.M.L.; writing—original draft, S.K., E.M.L., and J.C.R.; writing—review and editing, S.K., E.M.L., J.C.R., J.B., I.F.S., J.W. and D.L.W. All authors have read and agreed to the published version of the manuscript.

Funding: This research was funded by the Great Lakes Restoration Initiative and the U.S. Fish and Wildlife Service Recovery Challenge, grant number F21AC00707.

Institutional Review Board Statement: Ethical review and approval were waived for this study due to work with invertebrates.

Informed Consent Statement: Not applicable.

Data Availability Statement: Data for this study are available at https://doi.org/10.5066/P1AQGHWQ (accessed on 5 June 2024) [53].

Acknowledgments: We thank Randall Massey (University of Wisconsin-Madison) for TEM technical assistance.

Conflicts of Interest: The authors declare no conflicts of interest. The use of trade, firm, or product names is for descriptive purposes only and does not imply endorsement by the U.S. Government. The findings and conclusions in this article are those of the authors and the U.S. Geological Survey and do not necessarily represent the views of the U.S. Fish and Wildlife Service or the U.S. Environmental Protection Agency.

References

1. Graf, D.L.; Cummings, K.S. A 'big data' approach to global freshwater mussel diversity (Bivalvia: Unionoida), with an updated checklist of genera and species. *J. Molluscan Stud.* **2021**, *87*, eyaa034. [CrossRef]
2. Lopes-Lima, M.; Burlakova, L.E.; Karatayev, A.Y.; Mehler, K.; Seddon, M.; Sousa, R. Conservation of freshwater bivalves at the global scale: Diversity, threats and research needs. *Hydrobiologia* **2018**, *810*, 1–14. [CrossRef]

3. Downing, J.A.; Van Meter, P.; Woolnough, D.A. Suspects and evidence: A review of the causes of extirpation and decline in freshwater mussels. *Anim. Biodivers. Conserv.* **2010**, *33*, 151–185. [CrossRef]
4. Haag, W.R. Reassessing enigmatic mussel declines in the United States. *Freshw. Mollusk Biol. Conserv.* **2019**, *22*, 43–60. [CrossRef]
5. Wisconsin Mussel Species. Available online: https://wiatri.net/inventory/mussels/About/speciesList.cfm?theOrder=C (accessed on 14 August 2023).
6. Listed Species with Spatial Current Range Believed to or Known to Occur in Wisconsin. Available online: https://ecos.fws.gov/ecp/report/species-listings-by-state?stateAbbrev=WI&stateName=Wisconsin&statusCategory=Listed (accessed on 14 August 2023).
7. Wisconsin Endangered and Threatened Species Laws and List. Available online: https://p.widencdn.net/byxof6/ER001 (accessed on 14 August 2023).
8. Wisconsin Natural Heritage Working List. Available online: https://dnr.wisconsin.gov/sites/default/files/topic/NHI/NHIWorkingList.pdf (accessed on 14 August 2023).
9. The Clam Chronicle 2019 Spring. Available online: https://wiatri.net/inventory/mussels/news/pdf/2019Spring_ClamChronicle.pdf (accessed on 14 August 2023).
10. Bojko, J.; Reinke, A.W.; Stentiford, G.D.; Williams, B.; Rogers, M.S.J.; Bass, D. Microsporidia: A new taxonomic, evolutionary, and ecological synthesis. *Trends Parasitol.* **2022**, *38*, 642–659. [CrossRef]
11. Han, B.; Takvorian, P.M.; Weiss, L.M. Invasion of host cells by microsporidia. *Front. Microbiol.* **2020**, *11*, 172. [CrossRef]
12. Dunn, A.; Smith, J. Microsporidian life cycles and diversity: The relationship between virulence and transmission. *Microbes Infect.* **2001**, *3*, 381–388. [CrossRef]
13. Canning, E.U. Microsporidia. In *Parasitic Protozoa*, 2nd ed.; Kreier, J.P., Ed.; Academic Press, Inc.: San Diego, CA, USA, 1993; Volume 6, pp. 299–370.
14. Vávra, J.; Ronny Larsson, J.I. Structure of Microsporidia. In *Microsporidia: Pathogens of Opportunity*; Weiss, L.M., Becnel, J.J., Eds.; John Wiley & Sons, Inc.: Chichester, UK, 2014; pp. 1–70.
15. Cali, A.; Becnel, J.J.; Takvorian, P.M. Microsporidia. In *Handbook of the Protists*, 2nd ed.; Archibald, J.M., Simpson, A.G.B., Slamovits, C.H., Eds.; Springer International Publishing AG: Cham, Switzerland, 2017; pp. 1559–1618.
16. Canning, E.U.; Refardt, D.; Vossbrinck, C.R.; Okamura, B.; Curry, A. New diplokaryotic microsporidia (Phylum Microsporidia) from freshwater bryozoans (Bryozoa, Phylactolaemata). *Eur. J. Protistol.* **2002**, *38*, 247–265. [CrossRef]
17. Canning, E.U.; Okamura, B.; Curry, A. A new microsporidium, *Nosema cristatellae* n. sp. in the Bryozoan *Cristatella mucedo* (Bryozoa, Phylactolaemata). *J. Invertebr. Pathol.* **1997**, *70*, 177–183. [CrossRef]
18. Weng, M.; Zhang, J.; Li, A.; Zhang, Q.; Sato, H. Morphological and molecular characterization of a new microsporidium, *Janacekia tainanus* n. sp. from the adipose tissue of *Kiefferulus tainanus* (Diptera: Chironomidae) in China. *J. Invertebr. Pathol.* **2021**, *182*, 107578. [CrossRef]
19. Liu, X.; Ren, S.; Chen, Z.; Yin, Q.; Xiang, J.; Yu, J.; Li, D.; Zhang, J. *Jirovecia branchilis* n. sp. (Microsporidia) from glands of *Branchiura sowerbyi* (Oligochaeta: Tubificidae) in China. *Eur. J. Protistol.* **2023**, *88*, 125972. [CrossRef]
20. Morris, D.J.; Terry, R.S.; Ferguson, K.B.; Smith, J.E.; Adams, A. Ultrastructural and molecular characterization of *Bacillidium vesiculoformis* n. sp. (Microspora: Mrazekiidae) in the freshwater oligochaete *Nais simplex* (Oligochaeta: Naididae). *Parasitology* **2005**, *130*, 31–40. [CrossRef]
21. Knowles, S.; Leis, E.M.; Richard, J.C.; Cole, R.; Agbalog, R.E.; Putnam, J.G.; Goldberg, T.L.; Waller, D.L. A novel gonadotropic microsporidian parasite (*Microsporidium clinchi* n. sp.) infecting a declining population of pheasantshell mussels (*Actinonaias pectorosa*) (Unioinidae) from the Clinch River, USA. *Parasitologia* **2022**, *2*, 1–12. [CrossRef]
22. Bojko, J. Systematic identity and phylogenetic analysis of *Knowlespora clinchi* (Knowles et al. 2022) gen. et comb. nov. from pheasantshell mussels (*Actinonaiais pectorosa*). *J. Invertebr. Pathol.* **2022**, *194*, 107817. [CrossRef]
23. Liu, X.; Ren, S.; Chen, Z.; Yuan, X.; Song, R.; Yu, J.; Li, D.; Xiang, J.; Zhang, J. Two new species of *Bacillidium* (Microsporidia) from coelomocytes of *Branchiura sowerbyi* (Oligochaeta: Naididae) in China. *J. Invertebr. Pathol.* **2022**, *192*, 107785. [CrossRef]
24. Sapir, A.; Dillman, A.R.; Connon, S.A.; Grupe, B.M.; Ingels, J.; Mundo-Ocampo, M.; Levin, L.A.; Baldwin, J.G.; Orphan, V.J.; Sternberg, P.W. Microsporidia-nematode associations in methane seeps reveal basal fungal parasitism in the deep sea. *Front. Microbiol.* **2014**, *5*, 43. [CrossRef]
25. Liu, X.; Wen, M.; Zhao, Y.; Li, A.; Zhang, J. Morphological and molecular characterization of a new freshwater microsporidium, *Jirovecia sinensis* sp. n. (Microsporidia) infecting the coelomocytes of *Branchiura sowerbyi* (Oligochaeta: Naididae) in China. *J. Invertebr. Pathol.* **2020**, *173*, 107368. [CrossRef]
26. Morris, D.J.; Terry, R.S.; Adams, A. Development and molecular characterisation of the microsporidian *Schroedera airthreyi* n. sp. in a freshwater bryozoan *Plumatella* sp. (Bryozoa: Phylactolaemata). *J. Eukaryot. Microbiol.* **2005**, *52*, 31–37. [CrossRef]
27. Issi, I.V.; Tokarev, Y.S.; Seliverstova, E.V.; Voronin, V.N. Taxonomy of *Neoperezia chironomi* and *Neoperezia semenovaiae* comb. nov. (Microsporidia, Aquasporidia): Lessons from ultrastructure and ribosomal DNA sequence data. *Eur. J. Protistol.* **2012**, *48*, 17–29. [CrossRef]
28. Desser, S.S.; Koehler, A.; Barta, J.R.; Kamyab, J.; Ringuette, M.J. *Trichonosema algonquinensis* n. sp. (Phylum microsporidia) in *Pectinatella magnifica* (Bryozoa: Phylactolaemata) from Algonquin Park, Ontario, Canada. *J. Eukaryot. Microbiol.* **2004**, *51*, 389–393. [CrossRef]

29. Morris, D.J.; Adams, A. Development of *Schroedera plumatellae* gen. n., sp. n. (Microsporidia) in *Plumatella fungosa* (Bryozoa: Phylactolaemata). *Acta Protozool.* **2002**, *41*, 383–396.
30. Vossbrinck, C.R.; Andreadis, T.G.; Vavra, J.; Becnel, J.J. Molecular phylogeny and evolution of mosquito parasitic Microsporidia (Microsporidia: Amblyosporidae). *J. Eukaryot. Microbiol.* **2004**, *51*, 88–95. [CrossRef] [PubMed]
31. Cheney, S.A.; Lafranchi-Tristem, N.J.; Canning, E.U. Phylogenetic relationships of *Pleistophora*-like microsporidia based on small subunit ribosomal DNA sequences and implications for the source of *Trachipleistophora hominis* infections. *J. Eukaryot. Microbiol.* **2000**, *47*, 280–287. [CrossRef] [PubMed]
32. Nilsen, F. Small subunit rDNA phylogeny of *Bacillidium* sp. (Microspora, Mrazekiidae) infecting oligochaets. *Parasitology* **1999**, *118 Pt 6*, 553–558. [CrossRef] [PubMed]
33. Karpov, S.A.; Mamkaeva, M.A.; Aleoshin, V.V.; Nassonova, E.; Lilje, O.; Gleason, F.H. Morphology, phylogeny, and ecology of the aphelids (Aphelidea, Opisthokonta) and proposal for the new superphylum Opisthosporidia. *Front. Microbiol.* **2014**, *5*, 112. [CrossRef]
34. Tedersoo, L.; Sánchez-Ramírez, S.; Kõljalg, U.; Bahram, M.; Döring, M.; Schigel, D.; May, T.; Ryberg, M.; Abarenkov, K. High-level classification of the Fungi and a tool for evolutionary ecological analyses. *Fungal Divers* **2018**, *90*, 135–159. [CrossRef]
35. Balbiani, E. Sur les microsporidies ou psorospermies des articulés. *C. R. Acad. Sci.* **1882**, *95*, 1168–1171.
36. Vossbrinck, C.R.; Debrunner-Vossbrinck, B.; Weiss, L. Phylogeny of the microsporidia. In *Microsporidia: Pathogens of Opportunity*, 1st ed.; Weiss, L.M., Becnel, J.J., Eds.; John Wiley & Sons, Inc.: Chinchester, UK, 2014; pp. 203–220.
37. Voronin, V. On a macrotaxonomy of the phylum Microsporidia. *Parazitologiia* **2001**, *35*, 35–44. [PubMed]
38. Carella, F.; De Vico, G. Pathology, epidemiology, and phylogeny of mussel egg disease due to the microsporidian *Steinhausia mytilovum* (Field, 1924) in the Mediterranean mussel (*Mytilus galloprovincialis*). *J. Invertebr. Pathol.* **2023**, *198*, 107927. [CrossRef]
39. Nguyen, L.T.; Schmidt, H.A.; von Haeseler, A.; Minh, B.Q. IQ-TREE: A fast and effective stochastic algorithm for estimating maximum-likelihood phylogenies. *Mol. Biol. Evol.* **2015**, *32*, 268–274. [CrossRef]
40. Field, I.A. Biology and economic value of the sea mussel *Mytilus edulis*. *Bull. US Bur. Fish.* **1923**, *38*, 127–259.
41. Léger, L.; Hollande, A. Sur un nouveau protiste à facies de Chytridiopsis, parasite des ovules de l'huit. *CR Séanc. Soc. Biol.* **1917**, *80*, 61–64.
42. Farley, C.A. Neoplasms in estuarine mollusks and approaches ot ascertain causes. *Ann. N. Y. Acad. Sci.* **1977**, *298*, 225–232. [CrossRef] [PubMed]
43. Villalba, A.; Carballal, M.J.; López, M.C. *Pathologic Conditions of Three Carpet Shell Clam Species of Galicia (NW. of Spain), Proceedings of World Aquaculture '93—From discovery to commercialization, Torremolinos, Spain, 26–28 May 1993*; Carrillo, M., Ed.; European Aquaculture Society: Oostende, Belgium, 1993; p. 85.
44. Anderson, T.; Hine, P.; Lester, R. A *Steinhausia*-like infection in the ovocytes of Sydney rock oysters *Saccostrea commercialis*. *Dis. Aquat. Organ.* **1995**, *22*, 143–146. [CrossRef]
45. Carballal, M.J.; Iglesias, D.; Santamarina, J.; Ferro-Soto, B.; Villalba, A. Parasites and pathologic conditions of the cockle *Cerastoderma edule* populations of the coast of Galicia (NW Spain). *J. Invertebr. Pathol.* **2001**, *78*, 87–97. [CrossRef] [PubMed]
46. Comtet, T.; Garcia, C.; Le Coguic, Y.; Joly, J.P. Infection of the cockle *Cerastoderma edule* in the Baie des Veys (France) by the microsporidian parasite *Steinhausia* sp. *Dis. Aquat. Organ.* **2003**, *57*, 135–139. [CrossRef] [PubMed]
47. Silva, P.M.D.; Scardua, M.P.; Vieira, C.B.; Alves, A.C.; Dungan, C.F. Survey of pathologies in *Crassostrea gasar* (Adanson, 1757) oysters from cultured and wild populations in the São Francisco Estuary, Sergipe, Northeast Brazil. *J. Shellfish. Res.* **2015**, *34*, 289–296. [CrossRef]
48. Wadi, L.; Reinke, A.W. Evolution of microsporidia: An extremely successful group of eukaryotic intracellular parasites. *PLoS Pathog.* **2020**, *16*, e1008276. [CrossRef] [PubMed]
49. Sanders, J.L.; Lawrence, C.; Nichols, D.K.; Brubaker, J.F.; Peterson, T.S.; Murray, K.N.; Kent, M.L. Pleistophora hyphessobryconis (Microsporidia) infecting zebrafish *Danio rerio* in research facilities. *Dis. Aquat. Organ.* **2010**, *91*, 47–56. [CrossRef]
50. Geneious. Available online: www.geneious.com (accessed on 28 March 2024).
51. Altschul, S.F.; Gish, W.; Miller, W.; Myers, E.W.; Lipman, D.J. Basic local alignment search tool. *J. Mol. Biol.* **1990**, *215*, 403–410. [CrossRef]
52. National Library of Medicine National Center for Biotechnology Information. Available online: https://www.ncbi.nlm.nih.gov/genbank/ (accessed on 28 March 2024).
53. Knowles, S.; Leis, E.M.; Richard, J.C.; Standish, I.F.; Bojko, J.; Weinzinger, J.; Waller, D.L. *2018 Embarrass River Microsporidia: U.S. Geological Survey Data Release*; USGS Data Release Products: Madison, WI, USA, 2024. [CrossRef]

Disclaimer/Publisher's Note: The statements, opinions and data contained in all publications are solely those of the individual author(s) and contributor(s) and not of MDPI and/or the editor(s). MDPI and/or the editor(s) disclaim responsibility for any injury to people or property resulting from any ideas, methods, instructions or products referred to in the content.